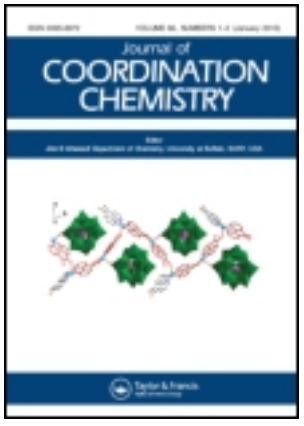

Journal of Coordination Chemistry
Publication details, including instructions for authors and subscription information:
http://www.tandfonline.com/loi/gcoo20

Synthesis, structure, NO donor activity of iron-sulfur nitrosyl complex with 2-aminophenol-2-yl and its antiproliferative activity against human cancer cells

N.A. Sanina[a], G.I. Kozub[a], O.S. Zhukova[b], N.S. Emel'yanova[a], T.A. Kondrat'eva[a], D.V. Korchagin[a], G.V. Shilov[a], N.S. Ovanesyan[a] & S.M. Aldoshin[a]

[a] Russian Academy of Sciences Institute of Problems of Chemical Physics, Chernogolovka, Russian Federation

[b] Russian Academy of Medical Sciences N.N. Blokhin Russian Cancer Research Center, Moscow, Russian Federation

Accepted author version posted online: 27 Sep 2013.Published online: 06 Nov 2013.

To cite this article: N.A. Sanina, G.I. Kozub, O.S. Zhukova, N.S. Emel'yanova, T.A. Kondrat'eva, D.V. Korchagin, G.V. Shilov, N.S. Ovanesyan & S.M. Aldoshin (2013) Synthesis, structure, NO donor activity of iron-sulfur nitrosyl complex with 2-aminophenol-2-yl and its antiproliferative activity against human cancer cells, Journal of Coordination Chemistry, 66:20, 3602-3618, DOI: 10.1080/00958972.2013.848980

To link to this article: http://dx.doi.org/10.1080/00958972.2013.848980

Journal of Coordination Chemistry, 2013
Vol. 66, No. 20, 3602–3618, http://dx.doi.org/10.1080/00958972.2013.848980

Synthesis, structure, NO donor activity of iron–sulfur nitrosyl complex with 2-aminophenol-2-yl and its antiproliferative activity against human cancer cells

N.A. SANINA*†, G.I. KOZUB†, O.S. ZHUKOVA‡, N.S. EMEL'YANOVA†, T.A. KONDRAT'EVA†, D.V. KORCHAGIN†, G.V. SHILOV†, N.S. OVANESYAN† and S.M. ALDOSHIN†

†Russian Academy of Sciences Institute of Problems of Chemical Physics, Chernogolovka, Russian Federation
‡Russian Academy of Medical Sciences N.N. Blokhin Russian Cancer Research Center, Moscow, Russian Federation

(*Received 30 May 2013; accepted 28 August 2013*)

A new tetranitrosyl binuclear iron complex, $[Fe_2(SC_6H_6N)_2(NO)_4]$ (**1**), has been synthesized by two methods. Molecular and crystalline structure of **1** were determined by X-ray analysis; the complex is binuclear of "μ-S" type with ~2.7052(4) Å between the irons. The compound crystallizes in monoclinic, space group $P2_1/n$, $Z = 2$; parameters of the unit cell: $a = 6.6257(2)$ Å, $b = 7.9337(2)$ Å, $c = 16.7858(4)$ Å, $\beta = 96.742(2)°$, $V = 876.26(4)$ Å^3. Parameters of Mössbauer spectrum for **1** are: isomer shift $\delta_{Fe} = 0.096(1)$ mm/s, quadrupole splitting $\Delta E_Q = 1.122(1)$ mm/s, line width 0.264 (1) mm/s at 293 K. As follows from the electrochemical analysis of aqueous solutions of **1**, it generates NO in protonic media without additional activation. NO amount and the rate of its activation are much higher in acidic solutions than in neutral and alkali ones. The constants of hydrolytic decomposition of **1** were calculated. The geometry and electronic structure of isolated **1** were studied using the density functional theory. Differential sensitivity of four lines of human tumor cells of various genesis to **1** has been determined (ovarian carcinoma (SCOV3), large intestine cancer (LS174T), mammary gland carcinoma (MCF7), and non-small cell carcinoma of lung (A549)); dependence of tumor cells amount on the complex concentration has been studied in order to use the complex as a promising antitumor agent for trials *in vivo*.

Keywords: Sulfur-nitrosyl iron complexes; X-ray analysis; MTT assay

1. Introduction

The search for new approaches to the development of effective and non-toxic "non-platinum" chemotherapeutic preparations based on metal coordination compounds has been intense [1]. Nitrosyl derivatives of biogenic iron are of a particular interest [2]. During the latest decade, nitric oxide (NO) was discovered to participate in carcinogenesis [3], in addition to its wide range of biological actions and ability to affect the organism systems,

*Corresponding author. Email: sanina@icp.ac.ru

fermentation activity, processes of cell fission, and death. Depending on NO local concentration *in vivo*, it can affect cell targets in different ways: the products of its reactions can either stimulate or, on the contrary, inhibit cancer growth. NO changes apoptosis level of tumor cells, activity of p53 gene, and neoplasm of vessels that nourish a tumor [4] and suppress activity of the key reparation protein of mammals O6-methyl-guanine-DNA-methyl-transferase [5]. Due to these properties, NO donors can be considered as a new class of anticancer agents [6]. However, available synthetic NO donors of different classes are not used as mono-therapeutic drugs for the treatment of oncological diseases, but for the activity boost of the existing chemotherapeutic preparations or radiotherapy [7–11]. That is why the search for new compounds, i.e. exogenous NO-donating drugs (NODD) that have direct antitumor effect, is of current importance [12–21].

Nitrosyl iron complexes (NIC) are intermediates in the decomposition of proteins and formation of S-nitrosothiols, which are catalyzed by the iron, and are reservoirs and transporters of NO *in vivo* [22, 23]. Based on these data, methods for synthesis and investigation of physical–chemical properties of synthetic analogs of NIC have been developed, with the aim to use them as NO donors in the monotherapy of oncological diseases. Recently, high anticancer activity has been shown for a series of iron nitrosyl complexes – synthetic models of the active sites of nitrosyl iron-sulfur proteins [24–26]. Functional sulfur-containing ligands in such NIC are reversible inhibitors for synthesis of cellular DNA, and they suppress the growth of tumors of various genesis, while the NO group, being the second component of the hybrid complex, is a key signal molecule that controls tumor growth.

The present work deals with synthesis, study of structure, and cytotoxic activity of a new NO donor, a representative of synthetic NIC of general composition $[Fe_2(\mu\text{-}SR)_2(NO)_4]$ (**1**), with R-2-aminothiophenol-2-yl, a structural analog of DNA pyridine bases belonging to the class of antimetabolites that inhibit the growth of malignant tumors of various genesis. The latter ones provide enhancement of the NO effect in the nitrosyl iron complex.

2. Experimental

2.1. *Materials and general methods*

All materials and solvents were purchased commercially and used as supplied, unless otherwise mentioned. Analytical grade solvents used for physical–chemical and *in vivo* studies were further purified by literature methods [27] before use.

2.2. *Instrumentation*

IR-spectrum (cm^{-1}) was recorded on Perkin–Elmer Spectrum 100X at room temperature. ^{57}Fe Mössbauer absorption spectra of polycrystals of **1** were recorded on WissEl operating in constant acceleration mode. ^{57}Co in Rh matrix was used as the source. Spectra at low temperatures were measured using continuous flow helium cryostat CF-506 (Oxford Instruments) with controllable temperature. Mössbauer spectra were processed by the least square method assuming the Lorentzian form of the individual spectral components.

2.3. *Preparation and characterization of the complex*

Complex **1** has been obtained by two methods.

Method 1. Polycrystals of **1** were obtained by the reported method [28]. 20 mL aqueous mixture of 0.3 g (7.5 mM) of KOH and 0.62 g (5 mM) of 2-aminothiophenol were added to 20 mL of aqueous solution of 0.496 g (2 mM) of $Na_2S_2O_3 \cdot 5H_2O$ and 0.57 g (1 mM) of $Na_2[Fe_2(S_2O_3)_2(NO)_4] \cdot 4H_2O$ obtained by the reported method [29] in an argon atmosphere within 20 min. The precipitate was separated by filtration and desiccated in air for 24 h. Fine-dispersed bright black crystals-bars were obtained by re-crystallization from acetonitrile. Yield: 75.5%.

Elemental analysis of polycrystals of **1** has been performed at the Analytical Center of IPCP RAS. Calcd for $Fe_2S_2C_{12}H_{12}N_6O_4$ (%): Fe – 23.30; S – 13.40; N – 17.50; C – 30.00; H – 2.50. Found (%): Fe – 23.29; S – 13.38; N – 17.48; C – 29.83; H – 2.46.

IR-spectrum (cm^{-1}) of **1**: 3523, 3456 (vw); 3367 (w); 3187, 3058, 3020, 2621, 2444, 1949, 1920 (vw); 1780, 1725 (vs); 1608 (s); 1562 (vw); 1512 (vw); 1474, 1448 (s); 1304, 1249 (m); 1160, 1146 (w); 1077, 1050 (vw); 1016 (w); 976, 946 (vw); 853 (w); 832, 754 (s); ν_{NO} 1780, 1725 cm^{-1}.

Method 2. Single crystals of **1** have been obtained in two steps under inert atmosphere [30].

Step 1. 1 g (3.2 mm) of bis-(2-nitrophenol-2-yl) disulfide in 50 mL of ethanol was reduced by 5 g (86.2 mm) of hydrazine hydrate. After complete dissolution of the initial disulfide in alcohol (30 min), the solution became red. Then the alcohol was removed by evaporation in vacuum, and hydrazinium salt of 2-nitrophenol-2-yl was isolated as water-soluble red oil.

Step 2. Mixture of solutions: 0.6 g (1 mM) of $Na_2[Fe_2(S_2O_3)_2(NO)_4] \cdot 4H_2O$ [29] in 20 mL of H_2O and 0.6 g (2.3 mM) of $Na_2S_2O_3 \cdot 5H_2O$ were placed in a three-necked flask in an argon atmosphere. 1 g (5.3 mM) of hydrazinium salt in 20 mL of H_2O was dripped under intense mixing. The reaction mixture was left in the refrigerator at temperature + 3 °C for 24 h. The precipitate was filtered through a porous glass filter N4, and washed thoroughly with several batches of absolute ether to separate a fraction containing an admixture phase. The deposit was dissolved in methylene chloride. Then methylene chloride was evaporated to the minimal volume and the solution was left in the freezer at –18 °C. 24 h later, black-red crystals of **1** were filtered from the solution. Yield of **1**, 20%. The ether fraction was evaporated in vacuum. Yield of the admixture powder, 35%.

Elemental analysis of the admixture powder was performed at the Analytical Center of IPCP RAS. Calcd for $Fe_2S_2C_{12}H_8N_6O_8$ (%): Fe – 20.68; S – 11.87; N – 15.55; C – 26.69; H – 1.49. Found (%): Fe – 20.36; S – 11.97; N – 15.11; C – 26.76; H – 1.68.

IR spectrum (cm^{-1}) of the admixture powder was recorded on Perkin–Elmer Spectrum 100X at room temperature: 3459, 3372 (vw); 3094, 3018, 2964, 2615, 2442 (vw); 1777, 1725 (vs); 1610 (w); 1590, 1566 (w); 1508 (s), 1474 (w), 1449 (w); 1337, 1306 (m); 1256 (w); 1161, 1148 (vw); 1106, 1040 (w); 959 (vw); 854 (w); 832, 804, 783, 752 (w); 731 (s); ν_{NO} 1777, 1725 cm^{-1}.

2.4. *X-ray analysis*

X-ray diffraction analysis of **1** was carried out on a CCD diffractometer Agilent XCalibur with EOS detector (Agilent Technologies UK Ltd., Yarnton, Oxfordshire, England). Data

collection, determination and refinement of the unit cell parameters were carried out using CrysAlis PRO program suite [31]. X-ray diffraction data were collected at 100(2) K using MoKα (λ = 0.71073 Å) radiation. Coverage of unique data was 95.2% complete to 75.6° (2θ). The structure was solved by direct methods. The positions and thermal parameters of non-hydrogen atoms were refined isotropically and then anisotropically by full-matrix least-squares. Selected crystallographic parameters and the data collection and refinement statistics are given in table 1. The bond lengths and angles in the structure of **1** are listed in table 2. All the hydrogen atom positions were located from the difference map. All calculations were performed with the SHELXTL program package [32].

The X-ray crystal structure data have been deposited with the Cambridge Crystallographic Data Center with reference code CCDC 932314. These data can be obtained free of charge via www.ccdc.cam.ac.uk/data_request/cif, by emailing data_request@ccdc.cam.ac.uk, or by contacting The Cambridge Crystallographic Data Center, 12 Union Road, Cambridge CB2 1EZ, UK; Fax: +44 1223 336033.

2.5. *Investigation*

Investigation of the polycrystalline powder of **1** obtained by method 1 was performed on powder X-ray difractometer ARLX'TRA (Thermo Electron Corporation).

Table 1. Crystal data and structure refinement for **1**.

Formula (fw)	$Fe_2S_2C_{12}H_{12}N_6O_4$ (480.1)
Temperature (K)	100(2)
Crystal system	Monoclinic
Space group	$P2_1/n$
Unit cell dimensions	
a (Å)	6.6257(2)
b (Å)	7.9337(2)
c (Å)	16.7858(4)
β (°)	96.742(2)
Volume (Å^3), Z	876.26(4), 2
Crystal size (mm)	0.1 × 0.2 × 0.25
Reflections collected/unique	15,330/4483 [R(int) = 0.0401]
Data/restraints/parameters	4483/0/142
Goodness of fit on F^2	1.016
Final R indices [$I > 2\sigma(I)$]	R_1 = 0.0352, wR_2 = 0.0733
R indices (all data)	R_1 = 0.0522, wR_2 = 0.0783
Largest diff. peak and hole (eÅ^{-3})	0.936 and −0.704

Table 2. Selected bond lengths [Å] and angles [°] for **1**.

Bond lengths (Å)			
Fe(1)–N(1)	1.671(1)	Fe(1)–N(2)	1.678(1)
N(1)–O(1)	1.176(2)	N(2)–O(2)	1.161(2)
Fe(1)–S(1)	2.2696(4)	Fe(1)–S(1A)	2.2748(4)
Fe(1)–Fe(1A)	2.7052(4)	S(1)–C(1)	1.783(1)
Bond angles (°)			
O(1)–N(1)–Fe(1)	170.6(1)	O(2)–N(2)–Fe(1)	171.9(1)
N(1)–Fe(1)–S(1)	109.60(4)	N(2)–Fe(1)–S(1)	107.36(4)
N(1)–Fe(1)–N(2)	118.37(6)	S(1)–Fe(1)–S(1A)	106.93(1)
C(1)–S(1)–Fe(1)	110.92(5)	C(1)–S(1)–Fe(1A)	109.25(5)

2.6. *Electrochemical determination of NO*

Sensor electrode "amiNO-700" of "inNO Nitric Oxide Measuring System" (Innovative Instruments, Inc., Tampa, FL, USA) was used for determination of the NO amount generated by **1** in solution. The NO concentration was recorded during ~500 s (with pace 0.2 s) in 1% DMSO aqueous solution with the NO donor concentration 0.1 μM. DMSO was purified according to reported procedure [27]. For calibration of the electrochemical sensor, a standard $NaNO_2$ aqueous solution (100 μM) was used, which was added to the mixture of 0.12 M of KI and 2 mL of 1 M H_2SO_4 in 18 mL of water. All experiments were performed in aerobic solutions at 250 °C and pH 6.5 (pH of solutions was measured by membrane pH-meter "HI 8314" (HANNA instruments, Germany).

2.7. *Quantum-chemical calculations*

Theoretical study of **1** was performed by density functional method in three approximations, i.e. using local functional BP86, hybrid functional B3LYP in the basis set 6–311++G**//6–31G* in the frame of program GAUSSIAN03 [33], and local functional PBE with SBK basis in the frame of program PRIRODA [34]. The absence of imaginary frequencies confirms stability of the structures. While comparing the energies of the optimized structures, the contribution of zero frequency energies was taken into account. To take into account solvation energies, polarizable continuum model (PCM) and extended basis set 6–311++G** were used (GAUSSIAN03 program).

2.8. *MTT Assay*

Cytotoxic activity of the complex was studied on lines of human tumor cells of various genes. Tumor cells were grown in RPMI 1640 medium containing 10% of calf embryonal serum and 5% of CO_2 at 37 °C. The cells were disseminated in 96-cavity plates and grown under similar conditions. Before the experiment, the compound was dissolved in 100 μL of dimethylsulfoxide (DMSO), then nutrient medium RPMI 1640 was used to get the desired concentration. The final concentration of DMSO in the samples was below 0.1% and did not affect the cell growth. Cytotoxic activity was determined from survival value of the cells in the samples. Survival test was performed using MTT test based on the ability of dehydrogenases of living cells to reduce achromatic MTT into blue crystals of formazan soluble in DMSO [35]. The complex (20 μL) was placed in the cavities with final concentrations of 100, 50, and 25 μM. The total incubation volume was 200 μL. The cells with the preparation were incubated under the above conditions for 72 h. After completion of the incubation, MTT reagent was added to the cells and under the same conditions incubation was performed for 2 h. Then, the formazan crystals were dissolved in 100 μL of DMSO during 20 min at 37 °C. Optical absorption of DMSO solutions was measured at an optical counter for multi-cell trays at wavelength 540 nm. The results (average values for 4 parallel measurements) were expressed as survival value in % (ex/control) × 100. A compound was considered active if cells survival value was equal to or less than 50% on one of three lines at concentration 100 μM ($IC_{50} \leq 100$ μM). The experimental error was below 5%.

3. Results and discussion

3.1. *Synthesis of the complex*

Polycrystals of **1** were obtained from replacement of thiosulfate ligands of the sodium salt of tetranitrosyl binuclear anion by the corresponding ligand – 2-aminophenol-2-yl (see method 1 in section 2), according to scheme 1.

1 is insoluble in water, poorly soluble in alcohols, and soluble in such solvents as CH_2Cl_2, acetonitrile, DMSO, acetone, $CHCl_3$, and tetrahydrofuran. Figure 1 shows polycrystals obtained by re-crystallization of the reaction product from acetonitrile.

Single crystals of **1** appropriate for X-ray analysis were obtained by method 2 (see section 2) according to scheme 2. In this method, distinct from method 1, hydrazinium salt of 2-nitrophenyl-2-thiolate, which was obtained as water soluble oil from the corresponding functional disulfide, is used for the replacement of thiosulfate ligands in $Na_2[Fe_2(S_2O_3)_2(NO)_4] \cdot 4H_2O$ by aromatic thiol.

In this method, conversion of the functional thiol to the salt is performed without using concentrated alkali solution. Alkalis are responsible for the formation of $Fe(OH)_3$ as a side product, thus leading to decrease of the target product yield. While synthesizing binuclear nitrosyl iron complex from hydrazinium salt of 2-nitropheno-2-yl, we intended to synthesize a new tetranitrosyl iron complex with NO_2 in the *ortho*-position of the aromatic ligand. However, the mixture of two tetranitrosyl iron complexes yields **1** (with 2-aminophenol-2-yl) and complex with 2-nitrophenol-2-yl. We assume that during the synthesis, the NO_2 group in the *ortho*-position is reduced by the hydrazinium salt (which is present in a 5-fold excess) in the presence of the iron salt. In organic compounds, the nitro group can be reduced to amine by hydrazine in the presence of metals, mainly Raney nickel [36, 37] and iron [38].

In the powder obtained by method 1, in addition to single crystals of **1**, binuclear nitrosyl iron complex with 2-nitrophenol as ligand was detected (its content can reach 50% in different experiments). The mixture of the complexes was separated by extraction with absolute ether (which easily dissolves the complex with 2-nitrophenol). Both fractions were identified by elemental analysis and IR-spectroscopy. IR-spectra of single crystals of **1** obtained by method 2 are similar to those of polycrystals obtained by method 1, and have a characteristic absorption of NH_2, 1608 cm^{-1}, and valence vibrations of NO, 1780, 1725 cm^{-1}. From elemental analysis and IR spectra of the admixture powder, we can assume that it is nitrosyl iron complex with 2-nitrophenol-2-yl (see section 2). The complex has characteristic absorptions for NO_2 (1508 cm^{-1}) and valence vibrations of NO, 1777, 1725 cm^{-1} (see figure 1 of Supplementary material).

To identify **1** obtained by method 1, diffraction patterns of polycrystal samples were recorded, which coincide with theoretical pattern for a single crystal of **1** synthesized by method 2. Polycrystals of **1** from method 1 were used for the physical–chemical and biological experiments.

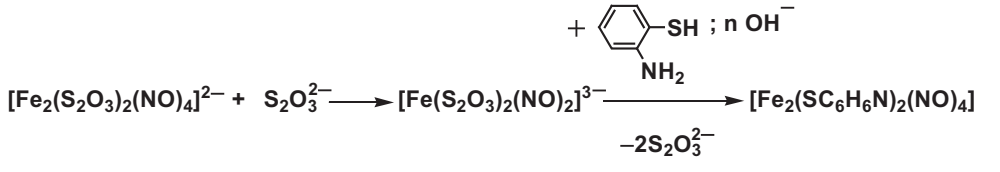

Scheme 1. '

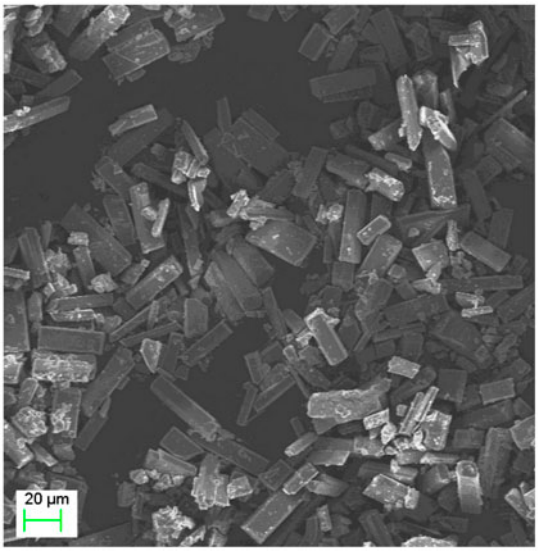

Figure 1. Polycrystals of **1** obtained by re-crystallization of the reaction product (scheme 1) from acetonitrile.

3.2. *IR studies*

In experimental spectra of polycrystals of **1** intense absorption of the NO (ν_{NO} = 1780, 1725 cm^{-1}) and at 1608 cm^{-1} typical for NH_2 are observed. However, in the spectrum of a single crystal of **1,** there is no absorption at 1500–1570 cm^{-1} typical for NO_2 of the initial disulfide.

3.3. *Mössbauer effect studies*

The Mössbauer spectrum of polycrystals of **1** is a doublet. Parameters of the Mössbauer spectrum at 293 K (quadrupole splitting ΔE_Q = 1.122(1) mm/s, isomer shift δ_{Fe} = 0.096 (1) mm/s and width of the absorption lines 0.264(1) mm/s) are close to those for neutral complexes with thiophenol, pyridil-2-yl [24], pyrimidil-2-yl [28], and 5-nitropyridine-2-yl [3]. This suggests structural similarity of two irons in **1** and the structure of nitrosyl complex with 2-aminophenol-2-yl with iron coordinated by two NO groups being linked with two bridging sulfurs. This is confirmed by X-ray data.

3.4. *Single-crystal X-ray diffraction*

From X-ray data, **1** has a centrosymmetric binuclear structure (figure 2) similar to that of anionic thiosulfate NIC $Q_2[Fe(S_2O_3)_2(NO)_4]$ with Q = Na, Me, Et, n-Pr, n-Bu [29, 39-41] and of neutral NIC $[Fe_2(\mu\text{-}SR)_2(NO)_4]$ with R = Me, Et, n-C_5H_{11}, CMe_3 [40–43], Py [44], Pym [28], and 5-nitroPy [30]. Interatomic Fe-Fe distance is 2.7052(4) Å, consistent with the presence of a chemical bond. Bond length C(1)-S(1) is 1.783(1) Å, equal, in the limits of accuracy, to similar bonds in µ-S binuclear complexes (see [24]), and exceeding the length of the double S = C bond (1.684 Å) [45]. This allows us to state that the thiol form of the ligand participates in the formation of this complex. The amino-group has a

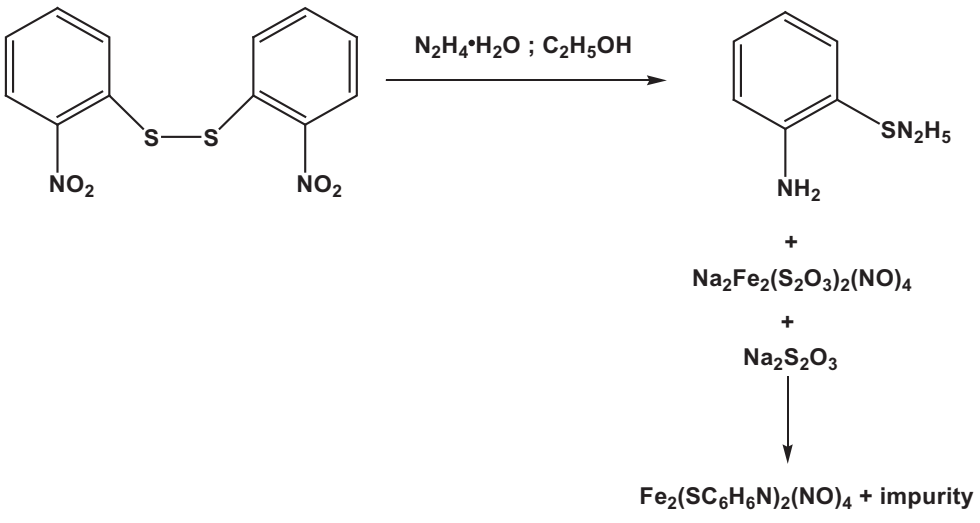

Scheme 2.

non-planar, pyramidal structure. N(3) deviates from the plane H(3A)C(2)H(3B) by 0.23 Å; the angle between the planes of the phenyl ring and NH_2 is 38.8°. Similar to the structure with pH substituent [46], the plane of the phenyl ring is almost perpendicular (89.8°) to the plane S(1)Fe(1)S(1A)Fe(1A), thus making impossible the presence of shortened intramolecular contacts of the NO group with 2-aminophenylthiol, as previously observed [30].

Similar to the compounds studied earlier [28, 30, 40–44], in **1** there are small differences in the structure of the NO groups, which leads to different Fe–N and N–O bond lengths and valence angles Fe–N–O (table 2).

Figure 3 shows the fragment of the crystalline structure projection on the crystallographic plane (YZ). Intermolecular contacts S(1)···H(3A) 2.81 Å, O(1)···H(6) 2.52 Å are shown by the dotted line. Intermolecular contacts of O(2) of the nitrosyl group with C(1) and C(2) atoms of the phenyl group of the adjacent complex (figure 4) point to the interaction of the lone pair of O(2) with the aromatic π-system. Consequently, C(1)–C(2) 1.410(2) and C(2)–C(3) 1.414(2) Å, which are the nearest to O(2), are elongated a little as compared to the other C–C bonds of phenyl (1.378(3)–1.399(2) Å). Interatomic interactions of O···π type were observed earlier in NIC and identified from the precision X-ray analysis [47].

3.5. *Study of NO donor activity of the complex in solutions*

Figure 5 shows experimental and theoretical time dependence of NO amount in solution upon complex **1** decomposition. In the protic media, the compound generates NO without thermo-, photo-, or fermentative activation. The kinetic dependences have maxima, which can be due to further NO conversion. We have used the simplest two-step scheme [28] for description of the process:

$$\mathrm{LFe(NO)} \xrightarrow{k_1} \mathrm{LFe} + \mathrm{NO}, \quad \text{where } \mathrm{L} = [\mathrm{Fe}(\mu_2 - \mathrm{SR})_2(\mathrm{NO})_3]$$

$$\mathrm{NO} \xrightarrow{k_2} \text{products},$$

which produces the following time dependence of NO concentration:

$$[\mathrm{NO}] = \frac{Ck_1}{k_2 - k_1}(e^{-k_1 t} - e^{-k_2 t})$$

Constant C is the maximum NO concentration in the absence of its further transformation. Values C, k_1, and k_2 were obtained by least squares from the experimental data (figure 6); for **1** k_1 and k_2 are 34.9×10^{-4} s^{-1} and 352.3×10^{-4} s^{-1}, respectively.

As follows from the experiments with pH increase from 6.5 to 8, the amount of NO generated by **1** decreases by a factor of four (table 3). Probably, the complex properties change under the action of hydroxide, though these processes should be examined additionally. From comparative analysis of the NO activity of **1** and the complex with phenolyl [48] in solutions at pH = 6.5 in anaerobic medium, **1** generates twice as much NO (~40 nM) as the latter (~20 nM). In aerobic solutions, the NO amount generated by phenolyl complex increases by five times (109 nM), while in **1** it almost does not change (~37 nM). **1** keeps rather high NO activity in DMSO solutions while storing in air. Figure 6 shows the experimental time dependence of NO generated upon decomposition of **1** in 1% aqueous DMSO solution. The measurements were performed during five hours, and each sample was taken from the basic solution every 30 min. For **1,** the maximum evolution of NO was observed at the very beginning and was constant during 30 min (~40 nM). Then NO amount decreased to 5 nM. For the phenolyl complex, NO donor activity upon storing reduces to

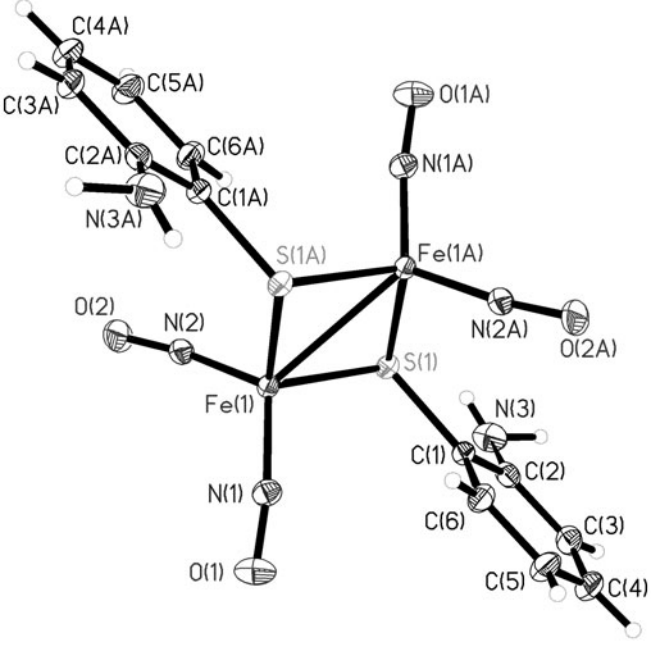

Figure 2. The general view of **1** with representation of atoms by thermal motion ellipsoids (p = 50%).

this value within an hour. Probably, in solutions of **1** stable nitrosyl intermediates exist, which are responsible for prolonged NO generation.

3.6. *Quantum-chemical calculations*

In table 4, the key parameters of the optimized geometry of **1** obtained by using various functionals are presented to compare them with the experimental data (table 2). All selected methods describe the structure of the complex satisfactorily. The complex is diamagnetic and its basic spin state should be singlet. However, for solutions obtained with B3LYP, the triplet state is lower by 16.6 kcal/M. On one hand, this can be a general overestimate of a high-spin state by hybrid functional [49]. It has been shown earlier [50] that the electronic structure of diamagnetic binuclear complexes of $[Fe_2(SR)_2(NO)_4]$ type corresponds to the opposite orientation of the spins of the unpaired electrons on each $Fe(NO)_2$ unit. Such state can be realized upon binding the spin 3/2 of Fe with the opposite-oriented spins S = 1/2 of two NO groups, and thus the triplet state has the correct spin structure (figure 7). Value of <S2> = 5.47 is also close to the theoretical value 6 for the electron configuration corresponding to three unpaired electrons on iron and one electron on each NO. With such approach, the singlet state could be realized provided the presence of several open shells, and it cannot be described in the framework of singlet-determinant approximation. A single-determinant state with distorted symmetry, with the spin density arising on each Fe and NO, can be an approximation to the accurate multi-determinant solution (figure 7).

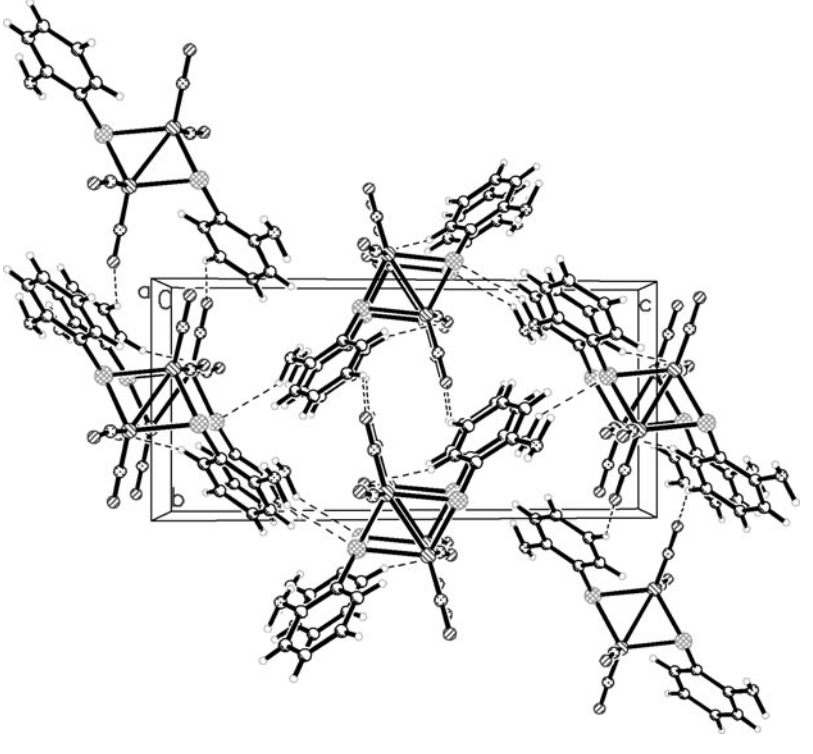

Figure 3. Fragment of the projection of the crystalline structure on the crystallographic plane (YZ).

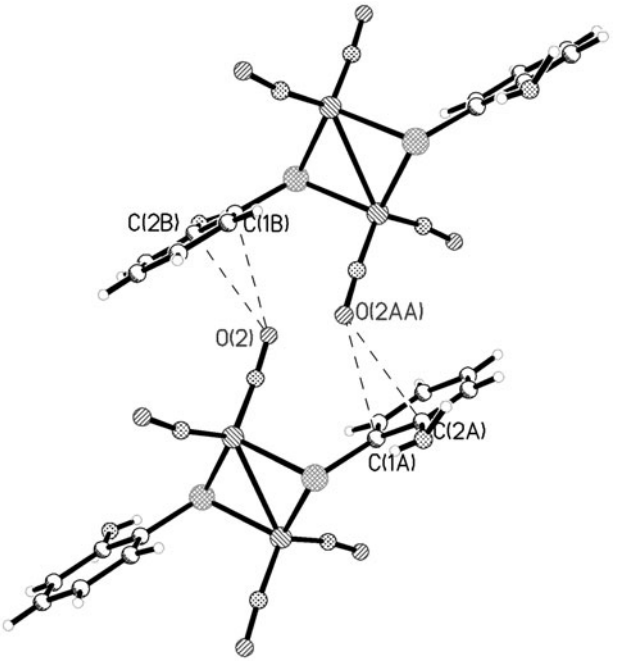

Figure 4. Intermolecular contacts of one of the nitrosyl groups with the π-system O(2)···C(2B) 3.00 Å, O(2)···C (1B) 3.14 Å.

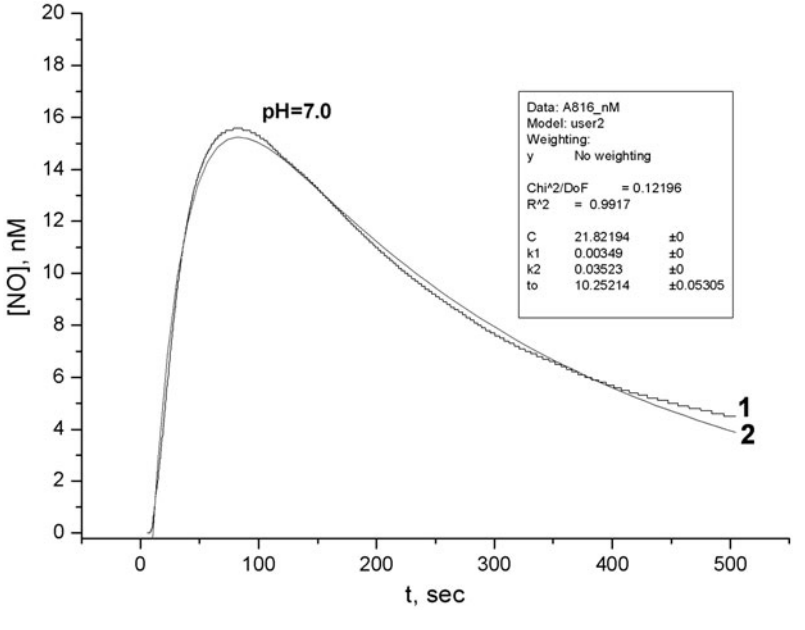

Figure 5. Experimental (1) and theoretical (2) time dependences of the NO amount generated in solution upon **1** decomposition in anaerobic 1% aqueous solution of DMSO at pH 7.0 and 25 °C.

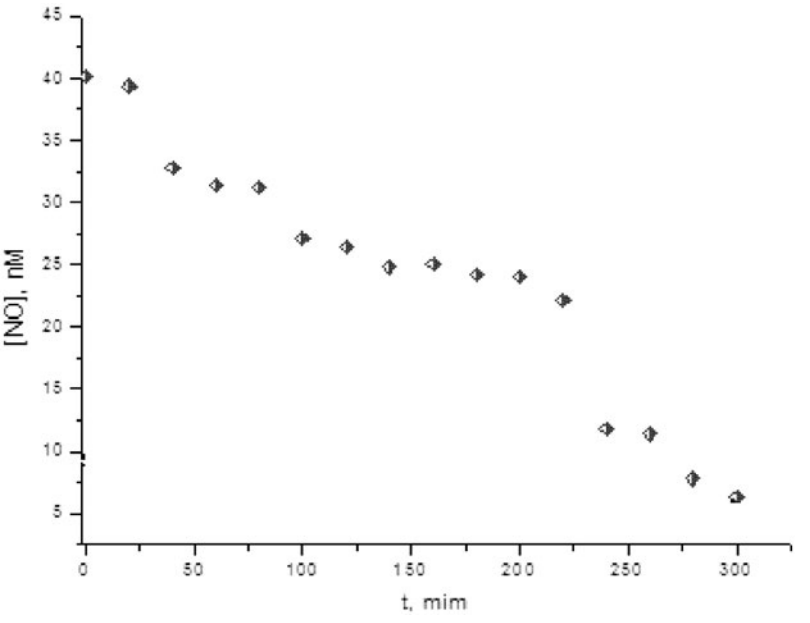

Figure 6. Time dependence of the NO amount generated by **1** (4×10^{-6}M l^{-1}) in anaerobic 1% aqueous solution of DMSO at 25 °C in distilled water at pH 6.5.

Distribution of the spin density (B3LYP/6–31G*) almost equally between Fe and two NO in the $Fe(NO)_2$ fragment points to the fact that a d orbital engaged by the unpaired electron does not have preferential localization either on the metal or on the ligand. Such molecular orbital can form from the orbitals of the metal and the NO ligands with close energetic characteristics. Residual two electrons on Fe and the electrons on the NO groups, which had opposite-oriented spins in the ground state, now engage two binding molecular orbitals Fe–NO, also of the delocalized type. Due to this delocalization, there is considerable contribution of ionic states $Fe^{3+}(NO^-)_2$ and $Fe^-(NO^+)_2$ in the wave function, responsible for increase of energy in the singlet state with filled shells.

Using quantum-chemical modeling, we examined the energy aspects of dissociation of the Fe–NO bond in **1**. The estimate was based on the difference of the energies of the initial complex and products upon escape of one NO in gaseous phase, as well as in water and DMSO. The effect of solvation in the polarized continuum model was taken into account [50, 51].

All approaches we have used lead, upon optimization of the geometry, to the structure presented in figure 8. Upon dissociation of the Fe–NO bond, a free coordination site arises

Table 3. Amount of NO generated by **1** at various pH in anaerobic conditions at T = 25 °C.

	NO amount, nM		
Complex	pH 6.5	pH 7.0	pH 8.0
1	40.8	15.6	9.4

Table 4. Selected optimized geometry parameters (bond lengths (Å), angles (°)) for **1**.

	B3LYP/6–31G* (triplet)	BP86/6–31G*	PBE/SBK
Fe1–N1	1.627 (1.727)	1.641	1.661
Fe1–N2	1.630 (1.731)	1.642	1.661
Fe1–S1	2.219 (2.397)	2.231	2.252
Fe1–S1A	2.226 (2.415)	2.242	2.252
N1–O1	1.171 (1.180)	1.187	1.172
N2–O2	1.169 (1.177)	1.191	1.172
S1–C1	1.782 (1.800)	1.793	1.779
Fe–Fe	2.606 (3.367)	2.608	2.664
N1–Fe1–N2	114.5 (115.5)	113.2	115.5
O1–N1–Fe1	166.0 (163.6)	166.2	168.1
O2–N2–Fe1	167.0 (166.0)	166.7	168.4

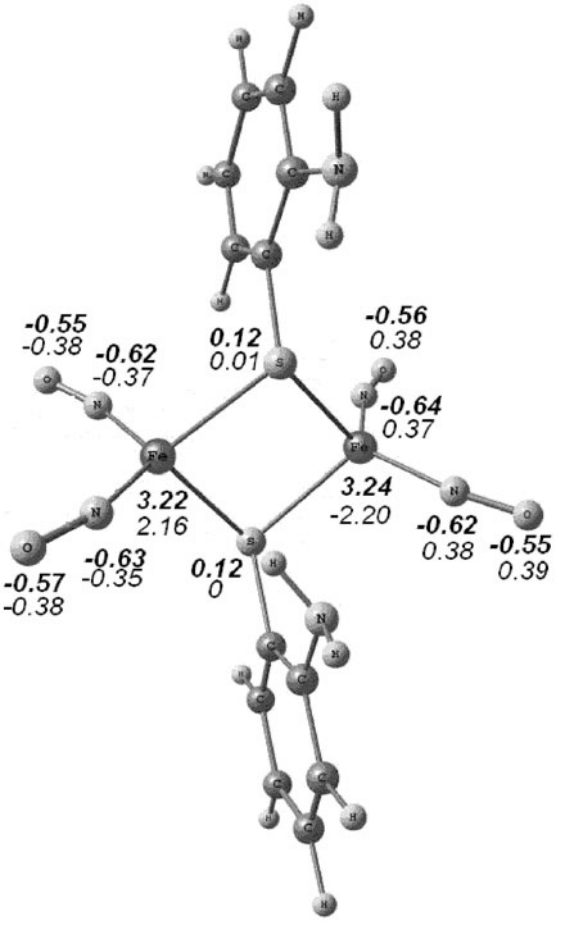

Figure 7. Distribution of the spin density in **1** (B3LYP/6–31G*). Bold type – triplet state, italics – singlet state with broken symmetry.

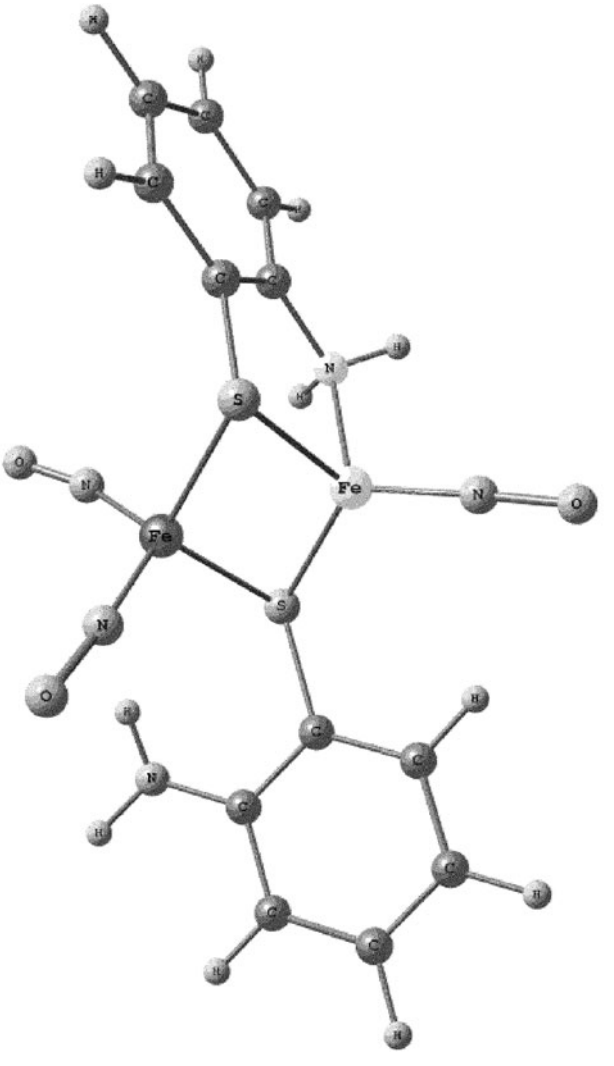

Figure 8. Theoretical structure forming upon NO separation from **1**.

in **1**. This results in the formation of intramolecular coordination bond Fe–N (2.10–2.13 Å), with nitrogen of NH_2 of the phenyl. This leads to stabilization of the forming structure and to decrease of its energy. The energy of NO separation from this complex was almost twice less than that for the complex with phenyl ligand [50] (table 5). Consequently, it should generate more NO in aqueous DMSO solution. Table 5 shows that in the condensed phase, the energy of separation decreases considerably for both complexes, thus pointing to the facility of this reaction in solutions and sufficient stability in air. All these data are in agreement with the experiment in solution, in which **1** generates twice as much NO as the complex with the phenyl ligand. On the other hand, formation of the stable structure upon separation of one NO should prevent further dissociation of the complex, consistent with

Table 5. Energy of NO separation.

	Energy of NO separation		
		Condensed phase	
Complex	Gaseous phase	H_2O	DMSO
1	−12.6	1.9	2.2
$[Fe_2(NO)_4(SPh)_2]$	−24.1	−8.7	−10.4

prolonged NO generation in DMSO solution under the conditions of the experiment (see section 3.5). Such NO generation is significant in anticancer therapy.

3.7. *Investigation of anti-proliferative activity of the complex*

Cytotoxic activity of **1** has been studied on four lines of human tumor cells: ovarian carcinoma (SCOV3), large intestine cancer (LS174T), mammary gland carcinoma (MCF7), and non-small cell carcinoma of lung (A549). **1** has different cytotoxic activity on the above cell lines (table 6) with the highest activity shown for A549 and SCOV3. Dependence of activity on concentration of **1** has been determined (table 7). The complex with phenolyl [25] exhibits maximum activity on the cells of myeloleukemia K562 (IC_{50} = 20 μM), and its activity is close to that of the platinum complex *cis*-DDP (IC_{50} = 20 μM). Lung carcinoma (A549) and ovarian carcinoma (SCOV3) are stable to the action of the phenolyl complex. Investigations of the phenolyl complex on transplantable tumors of mice Ca-755 and melanoma B-16 (mice are the first generation hybrids BDF_1 ($C_{57}Bl/6$ x $DBA/_2$) and $DBA/_2$, weight 18–25 g, obtained in the animal laboratory of N.N. Blokhin Russian Cancer Research Center of RAMS) showed a moderate statistically important anticancer effect when administered intra-abdominally during 5 days in 10–75 mg/kg dose as compared to the control experiments. Toxicity of the complex was much lower (LD_{100} = 60 mg/kg) than that of cisplatin (LD_{100} = 16 mg/kg).

Table 6. IC_{50} values (μM, for **1** on the lines of human tumor cells).

Complex	SKOV3	LS174T	MCF7	A549
1	27	37	74	25

Table 7. Dependence of survival of tumor cells on the concentration of **1**.

	Survival (%)			
	Concentration (μM)			
Cells	25	50	100	IC_{50} (μM)
MCF7	100	24.3	12.5	37
SCOV3	52	6.3	6.9	27
LS174T	100	83.6	13.9	74

From the above data on cytotoxic activity, we suggest that the complex with 2-aminophenolyl is a more promising anticancer agent for testing *in vivo* as a prolonged-release NO donor compared to the complex with phenolyl.

4. Conclusion

Single crystals of nitrosyl iron complex with sulfur-containing ligand 2-aminophenol-2-yl, which is a structural analog of DNA thiopyridine base, have been synthesized; their molecular and crystalline structure have been studied by X-ray method, and the electron structure has been determined by quantum chemistry and Mössbauer spectroscopy. The use of a sulfur-containing ligand with the amino-group in the *ortho*-position of the phenyl ring was shown to yield the nitrosyl iron complex with prolonged NO generation in aqueous solutions and with a wider range of cytotoxic activities compared to the nitrosyl iron complex with thiophenol studied earlier.

Supplementary material

Supplemental data for this article can be accessed http://dx.doi.org/10.1080/00958972.2013.848980.

Acknowledgments

The work has been supported by the Program of the Presidium of RAS "Fundamental sciences for medicine."

References

[1] J.C. Dabrowiak. *Metals in Medicine*, p. 342 *John Wiley & Sons*, (2009).
[2] R.L. Elliott, J.F. Head. *J. Cancer Therapy*, **3**, 278 (2012).
[3] S. Moccelin. *Curr. Cancer Drug Targets*, **9**, 214 (2009).
[4] B. Brune, N. Scheneiderhan. *Toxicol. Lett.*, **193**, 19 (2003).
[5] L. Liu, M. Xu-Welliver, S. Kanugula, A.E. Pegg. *Cancer Res.*, **62**, 3037 (2002).
[6] D. Wink., J. Vodovoz, J. Cook. Biochemistry, **63**, 948 (1998).
[7] N.P. Konovalova, S.A. Goncharova, L.M. Volkova, T.A. Raevskaya, L.T. Eremenko, A.M. Korolev. *Nitric Oxide*, **8**, 59 (2003).
[8] W. Yang, P.A. Rogers, H. Ding. *J. Biol. Chem.*, **277**, 12868 (2002).
[9] O. Siri, A. Tabard, P. Pullumbi, R. Guilard. *Inorg. Chim. Acta*, **350**, 633 (2003).
[10] J.L. Burgaud, E. Jngini, P. Del Soldato, N.Y. Ann. *Acad. Sci.*, **962**, 360 (2002).
[11] T.I. Karu, L.V. Pyatibrat, G.S. Kalendo. *Toxicol. Lett.*, **121**, 57 (2001).
[12] A. Millet, A. Bettaieb, F. Renaud, L. Prevotat, A. Hammann, E. Solary, B. Mignotte, J.F. Jeannin. *Gastroenterology*, **123**, 235 (2002).
[13] V.J. Findlay, D.M. Townsend, J.E. Saavedra, G.S. Buzard, M.L. Citro, L.K. Keefer, X. Ji, K.D. Tew. *Mol. Pharmacol.*, **65**, 1070 (2004).
[14] S.L. Pan, J.H. Guh, C.Y. Peng, S.W. Wang, Y.L. Chang, F.C. Cheng, J.H. Chang, S.C. Kuo, F.Y. Lee, C.M. Teng. *J. Pharmacol. Exp. Ther.*, **314**, 35 (2005).
[15] E.J. Yeo, Y.S. Chun, Y.S. Cho, J. Kim, J.C. Lee, M.S. Kim, J.W. Park. *J. Natl. Cancer Inst.*, **95**, 516 (2003).
[16] B. Rigas, K. Kashfi. *Trends Mol. Med.*, **10**, 324 (2004).
[17] J.L. Williams, S. Borgo, I. Hasan, E. Castillo, F. Traganos, B. Rigas. *Cancer Res.*, **61**, 3285 (2001).

[18] C. Levagna, P. Del Soldato, J.L. Burgaud, P. Rampal. *Curr. Cancer Drug Targets*, **3**, 407 (2003).
[19] J.L. Williams, N. Nath, J. Chen, T.R. Hundley, J. Gao, L. Kopelovich, K. Kashfi, B. Rigas. *Cancer Res.*, **63**, 7613 (2003).
[20] Y.J. Lee, K.H. Lee, J.M. Jessup, D.W. Seol, T.H. Kim, T.R. Billar, Y.K. Song. *Oncogene*, **20**, 1476 (2001).
[21] M. Chawla-Sarkar, J.A. Bauer, J.A. Lupica, B.H. Morrison, Z. Tang, R.K. Oates, A. Almasan, J.A. DiDonato, E.C. Borden, D.J. Lindner. *J. Biol. Chem.*, **278**, 39461 (2003).
[22] A.R. Butler, I.I. Megson. *Chem. Rev.*, **102**, 1155 (2002).
[23] H. Lewandowska, M. Kalinowska, K. Brzoska, K. Wojciuk, G. Wojciuk, M. Kruszewski. *Dalton Trans.*, **40**, 8273 (2011).
[24] N.A. Sanina, S.M. Aldoshin *Russ. Chem. Bull. (Engl. Transl.)*, **60**, 1223 (2011).
[25] N.A. Sanina, O.S. Zhukova, S.M. Aldoshin, N.S. Emel'yanova, G.K. Gerasimova. *Patent RU* 2429242, (2011).
[26] N.A. Sanina, K.A. Lysenko, O.S. Zhukova, T.N. Roudneva, N.S. Emelyanova, S.M. Aldoshin, *Patent US* 8,067,628 B2 (2011).
[27] A. Weissberger, E. Proskauer, J.A. Riddick, E.E. Toops. *Organic Solvents: Physical Properties and Methods of Purification*, Interscience Publishers Inc., New York (1955).
[28] N.A. Sanina, G.V. Shilov, S.M. Aldoshin, A.F. Shestakov, L.A. Syrtsova, N.S. Ovanesyan, E.S. Chudinova, N.I. Shkondina, N.S. Emel'yanova, A.I. Kotel'nikov. *Russ. Chem. Bull. (Engl. Transl.)*, **58**, 572 (2009).
[29] N.A. Sanina, S.M. Aldoshin, T.N. Rudneva, N.I. Golovina, G.V. Shilov, Yu. M. Shul'ga, V.M. Martynenko, N.S. Ovanesyan, *Russ. J. Coord. Chem.*, **31**, 301 (2005).
[30] G.I. Kozub, N.A. Sanina, T.A. Kondrat'eva, G.V. Shilov, D.V. Korchagin, N.S. Ovanesyan, S.M. Aldoshin, *Russ. J. Coord. Chem.*, **38**, 671 (2012).
[31] Agilent. *CrysAlis PRO (Version 171.35.19)*, Agilent Technologies UK Ltd, Yarnton, Oxfordshire, England (2011).
[32] G.M. Sheldrick. *SHELXTL (Version 6.14)*, Structure Determination Software Suite, Bruker AXS, Madison, Wisconsin, USA (2000).
[33] M.J. Frisch, G.W. Trucks, H.B., Schlegel, G.E. Scuseria, M.A. Robb, J.R. Cheeseman, J.A. Montgomery Jr., T. Vreven, K.N. Kudin, J.C. Burant, J.M. Millam, S.S. Iyengar, J. Tomasi, V. Barone, B. Mennucci, M. Cossi, G. Scalmani, N. Rega, G.A. Petersson, H. Nakatsuji, M. Hada, M. Ehara, K. Toyota, R. Fukuda, J. Hasegawa, M. Ishida, T. Nakajima, Y. Honda, O. Kitao, H. Nakai, M.L.X. Klene, J.E. Knox, H.P. Hratchian, J.B. Cross, C. Adamo, J. Jaramillo, R. Gomperts, R.E. Stratmann, O. Yazyev, A.J. Austin, R. Cammi, C. Pomelli, J.W. Ochterski, P.Y. Ayala, K. Morokuma, G.A. Voth, P. Salvador, J.J. Dannenberg, V.G. Zakrzewski, S. Dapprich, A.D. Daniels, M.C. Strain, O. Farkas, D.K. Malick, A.D. Rabuck, K. Raghavachari, J.B. Foresman, J.V. Ortiz, Q. Cui, A.G. Baboul, S. Clifford, J. Cioslowski, B.B. Stefanov, G. Liu, A. Liashenko, P. Piskorz, I. Komaromi, R.L. Martin, D.J. Fox, T. Keith, M.A. Al-Laham, C.Y. Peng, A. Nanayakkara, M. Challacombe, P.M.W. Gill, B. Johnson, W. Chen, M.W. Wong, C. Gonzalez, J.A. Pople. *Gaussian 03 Revision D.01*, Gaussian Inc., Wallingford, CT (2004).
[34] D.N. Laikov. *Chem. Phys. Lett.*, **81**, 151 (1997).
[35] O.S. Zhukova. *Russ. Biother. J.*, **3**, 12 (2004).
[36] Organicum. *Practical work on organic chemistry*, Vol. 2, p. 224 Mir, Moscow (1979).
[37] V.A. Reznikov. *Chemistry of nitrogen-containing compounds*, p. 75, NSU, Novosibirsk (2006). K. Veigand, *Experimental methods in organic chemistry*, Vol. 1, p. 346, Khimiya, Moscow (1968).
[38] A.Kh. Shakhnes, S.S., Vorob'ev, S.A. Shevelev. *Russ. Chem. Bull.*, **55**, 938 (2006)
[39] N.A. Sanina, O.A. Rakova, S.M. Aldoshin, I.I. Chuev, E.G. Atovmyan, N.S. Ovanesyan. *Russ. J. Coord. Chem.*, **27**, 179 (2001).
[40] C. Glidewell, R.J. Lambert, N.B. Hursthouse, M. Motevalli. *J. Chem. Soc., Dalton Trans.*, 1989 (2061).
[41] J.T. Thomas, J.H. Robertson, E.G. Cox. *Acta Crystallogr.*, **11**, 599 (1958).
[42] C. Glidewell, M.E. Harman, M.B. Hursthouse, I.L. Johnson, M. Motevalli. *J. Chem. Res. (S)*, **212**, 1676 (1988).
[43] O.A. Rakova, N.A. Sanina, G.V. Shilov, Yu. M. Shul'ga, V.M. Martynenko, N.S. Ovanesyan, S.M. Aldoshin. *Russ. J. Coord. Chem.*, **28**, 341 (2002).
[44] N.A. Sanina, L.A. Syrtsova, N.I. Shkondina, E.S. Malkova, A.I. Kotelnikov, S.M. Aldoshin. *Russ. Chem. Bull. (Engl. Transl.)*, **56**, 761 (2007).
[45] J. Jolley, W.I. Cross, R.G. Pritchard, C.A. McAuliffe, K.B. Nolan. *Inorg. Chim. Acta*, 315 (2001).
N.A. Sanina, N.S. Emel'yanova, A.N. Chekhlov, A.F. Shestakov, I.V. Sulimenkov, S.M. Aldoshin. *Russ. Chem. Bull. (Engl. Transl.)*, **59**, 1126 (2010).
[47] S.M. Aldoshin, K.A. Lysenko, MYu Antipin, N.A. Sanina, V.V. Gritsenko. *J. Mol. Struct.*, **875**, 309 (2008).
[48] T.S. Stupina, I.I. Parkhomenko, I.V. Balalaeva, G.V. Kostyuk, N.A. Sanina. A.A. Terent'ev, *Russ. Chem. Bull. (Engl. Transl.)*, **60**, 1488 (2011).
[49] M. Radon, M. Srebro, E. Broclawik. *J. Chem. Theory Comput.*, **5**, 1237 (2009).
[50] A.F. Shestakov, Yu.N. Shul'ga, N.S. Emel'yanova, N.A. Sanina, S.M. Aldoshin. *Russ. Chem. Bull.*, **55**, 2133 (2006).
[51] N.S. Emel'yanova, A.F. Shestakov, I.V. Sulimenkov, T.N. Rudneva, N.A. Sanina, S.M. Aldoshin. *Russ. Chem. Bull. (Engl. Transl.)*, **61**, 1 (2012).